Violation of the fluctuation-dissipation theorem in confined driven colloids

R.Mauri[1] (*) and D.Leporini[2,3](**)

[1] *Dipartimento di Ingegneria Chimica, DICCISM, Universita' di Pisa, I-56126 Pisa, Italy*

[2] *Dipartimento di Fisica "Enrico Fermi", Universita' di Pisa, Largo B.Pontecorvo 3, I-56127 Pisa, Italy*

[3] *SOFT-INFM-CNR, P.zza A. Moro 2, I-00185, Roma, Italy*

PACS. `05.40.-a` – Fluctuation phenomena, random processes, noise, and Brownian motion.

Abstract. – Analytical models describing a colloidal particle confined in a harmonic well, **e.g. provided by an optical trap,** and driven by shear flows are presented. Violation of both static and dynamic fluctuation-dissipation theorem (FDT) is clearly seen, thus clarifying the connection between such FDT violation and the breakdown of the detailed balance. The simple shear and Taylor-Couette velocity fields are studied in detail, showing that loosening confinement enhances FDT violations. In addition, cases violating FDT but not energy equipartition are presented. For the cases under study, an effective temperature is defined via the static FDT, which appears to be more **physically sound** than the one defined via the time-dependent FDT. **Confining sheared colloidal particles by optical tweezers yields considerable FDT violation** .

The violation of the fluctuation-dissipation theorem (FDT) and the possible extension of thermodynamics when the system is out-of equilibrium, specifically the existence of a non-equilibrium temperature [1, 2], has attracted recent theoretical [3–8], numerical [9, 10] and experimental [11,12] interest. In particular, sheared systems [3,9,10,13] **and stationary flows** [4] have been studied intensively with particular reference to the non-equilibrium properties of colloidal suspensions [11,12,14]. In the present paper, the role played by confinement in FDT violation **and its relationship with the breakdown of the detailed balance** [6, 7] is discussed, by studying in detail some simple models describing one colloidal particle confined in a harmonic well and under antagonistic driving by two different velocity profiles: pure shear and Taylor-Couette flows.

First, the necessary background on FDT is summarized [8]. Let us consider a system of interest and denote with $\langle A\rangle_0$ the canonical average of the observable A over the configurations $\mathcal{C}$ of the unperturbed system in equilibrium at temperature T. At time $t = 0$, a constant small perturbation coupled to the observable $B(\mathcal{C})$ is applied to the system, shifting its energy by an amount $-\varepsilon B(\mathcal{C})$. This perturbation is used to investigate the linear response property of the

(*) E-mail: `r.mauri@ing.unipi.it`
(**) E-mail: `dino.leporini@df.unipi.it`

system and drives the expectation value $\langle A(t)\rangle_\varepsilon$ of the observable $A(\mathcal{C})$, not necessarily equal to $B(\mathcal{C})$, from its equilibrium value, $\langle A(t=0)\rangle_\varepsilon = \langle A\rangle_0$, towards a new equilibrium value, $\langle A\rangle_\varepsilon$. Here $\langle A(t)\rangle_\varepsilon$ denotes the expectation value of the observable $A(t)$ over all the possible dynamical paths originating from the initial equilibrium configurations, weighted with the canonical probability distribution. If we define the correlation function and time-dependent susceptibility as

$$C_{A,B}(t,s) = \langle A(t)\,B(s)\rangle_0, \tag{1}$$

$$\chi_{A,B}(t) = \lim_{\varepsilon\to 0}\frac{\langle A(t)\rangle_\varepsilon - \langle A(t)\rangle_0}{\varepsilon}, \tag{2}$$

the integrated form of the FDT theorem states that

$$\chi_{A,B}(t) = \frac{1}{k_B T}\left[C_{A,B}(t,t) - C_{A,B}(t,0)\right], \tag{3}$$

k_B being the Boltzmann constant. The static form of the FDT is obtained from Eq. (3) in the limit $t\to\infty$. In this case, $\chi_{AB} = \left[\partial\langle A\rangle_\varepsilon/\partial\varepsilon\right]_{\varepsilon=0}$, $C_{A,B}(t,t)\to\langle AB\rangle_0$ while $C_{A,B}(t,0)\to\langle A\rangle_0\langle B\rangle_0$, so that Eq. (3) reduces to

$$\chi_{AB} = \frac{1}{k_B T}\left[\langle AB\rangle_0 - \langle A\rangle_0\langle B\rangle_0\right] \tag{4}$$

Henceforth, for clarity sake the subscript "0" in the ensemble average will be understood.

Model. – Consider a very dilute suspension of spherical particles with radius a, immersed in an incompressible fluid having temperature T, density ρ and viscosity η. Assume that hydrodynamic particle-particle and particle-wall interactions can be neglected, with the suspended particles moving with low velocities $\mathbf{V}$, so that the Reynolds number $N_{Re} = \rho V a/\eta$ is low and inertia may be neglected. Accordingly, in the absence of any external force, the velocity of the particle at any position $\boldsymbol{x} = (x,y,z) = (x_1,x_2,x_3)$ equals that of the fluid, $\boldsymbol{v}$, which, here, is assumed to be a shear flow, $\boldsymbol{v} = \boldsymbol{\kappa}\cdot\boldsymbol{x}$, where $\boldsymbol{\kappa}$ is the velocity gradient tensor. In addition, let us assume that the suspended particle is subjected to a harmonic force field, $\phi(\mathbf{x}) = K_{ij}x_ix_j$, where the $\mathbf{K}$ matrix is symmetric and positive definite. Therefore, the force $\boldsymbol{F}$ exerted upon the suspended particle depends on the particle location $\boldsymbol{x}$ only and is the sum of the drag force, $\zeta\mathbf{v}$, with $\zeta = 6\pi\eta a$ denoting the drag coefficient, and the harmonic force, $-\boldsymbol{\nabla}\phi$, i.e.,

$$\boldsymbol{F}(\boldsymbol{x}) = -\boldsymbol{\Gamma}\cdot\boldsymbol{x}, \tag{5}$$

where

$$\boldsymbol{\Gamma} = \boldsymbol{K} - \zeta\boldsymbol{\kappa}. \tag{6}$$

The $\boldsymbol{\Gamma}$ matrix is sometimes referred to as the damping matrix and, together with Eq. (7) defines an Ornstein-Uhlenbeck process (OU) [17].

The probability $P(\boldsymbol{x},t)$ to find the particle at location $\boldsymbol{x}$ at time t satisfies the Smoluchowski equation, [16]

$$\frac{\partial P}{\partial t} + \frac{1}{\zeta}\boldsymbol{\nabla}\cdot\left[\boldsymbol{F}(\boldsymbol{x})\,P - k_B T\boldsymbol{\nabla}P\right] = \delta(\boldsymbol{x}-\boldsymbol{x}_0)\,\delta(t), \tag{7}$$

which can be easily derived from the Fokker-Planck equation, considering the expression $D = k_B T/\zeta$ for the molecular diffusivity. The general solution of Eq. (7) is given by the conditional probability:

$$P(\boldsymbol{x},t|\boldsymbol{x}_0,0) = \mathcal{N}exp\left[-\frac{1}{2}\left(\boldsymbol{x}-\langle\boldsymbol{x}(t)\rangle\right)^T\cdot\boldsymbol{\sigma}(t)^{-1}\cdot\left(\boldsymbol{x}-\langle\boldsymbol{x}(t)\rangle\right)\right], \tag{8}$$

where $\langle \boldsymbol{x}\,(t=0)\rangle = \boldsymbol{x}_0$, $\mathcal{N}$ is a normalization factor and $\langle \boldsymbol{x}\,(t)\rangle = \boldsymbol{G}\,(t)\cdot\boldsymbol{x}_0$, where $\boldsymbol{G}\,(t) = exp\,(-\boldsymbol{\Gamma}t/\zeta)$ defines a proper Green function. The correlation matrix $\boldsymbol{\sigma}\,(t)$ with elements $\sigma_{ij}(t) = \langle [x_i\,(t) - \langle x_i\,(t)\rangle]\,[x_j\,(t) - \langle x_j\,(t)\rangle]\rangle$ follows from [17]

$$\boldsymbol{\sigma}\,(t) = \frac{2k_BT}{\zeta}\int_0^t \boldsymbol{G}\,(t')\cdot{}^t\boldsymbol{G}\,(t')\,dt', \tag{9}$$

where ${}^t\boldsymbol{X}$ denotes the transpose of $\boldsymbol{X}$. If all real parts of the eigenvalues of the damping matrix $\boldsymbol{\Gamma}$ are larger than zero, a stationary solution of Eq. (8) exists, with $\langle \boldsymbol{x}(\infty)\rangle = 0$ and $\boldsymbol{\sigma} = \boldsymbol{\sigma}(\infty)$. In that case, one finds [17]:

$$(\boldsymbol{\Gamma}\cdot\boldsymbol{\sigma})^{sym} = k_BT\boldsymbol{I}, \tag{10}$$

where $\boldsymbol{X}^{sym} = (\boldsymbol{X} + {}^t\boldsymbol{X})/2$ denotes the symmetric part of the matrix $\boldsymbol{X}$ and $\boldsymbol{I}$ is the identity matrix. The particular case of a symmetric $\boldsymbol{\Gamma}$ matrix is of special interest. It ensures *detailed balance* and the *conservative* character of the force $\boldsymbol{F}^{OU}(\boldsymbol{x})$ [17]. In this case, Eq. (10) yields $\boldsymbol{\sigma} = k_BT\boldsymbol{\Gamma}^{-1}$.

The correlation function (1) for $\tau \geq 0$ and $A = x_i, B = x_j$ is evaluated in terms of a regression theorem as [17]:

$$C_{i,j}(t+\tau,t) = \sum_k G_{ik}(\tau)\,\sigma_{kj}(t), \tag{11}$$

where $C_{i,j} = C_{x_i,x_j}$. Let us define the susceptibility $\chi_{ij}\,(t) = \chi_{x_i,x_j}\,(t)$ for $t > 0$ via the relation $\langle \boldsymbol{x}\,(t)\rangle_\varepsilon = \boldsymbol{\chi}\,(t)\cdot\boldsymbol{\varepsilon}$, where $\langle \boldsymbol{x}\,(t)\rangle_\varepsilon$ is the displacement due the applied (small) step force $\boldsymbol{\varepsilon}\,(t) = \boldsymbol{\varepsilon}$ for $t > 0$ and zero otherwise. In addition, $\langle \boldsymbol{x}\,(t)\rangle_\varepsilon$ is derived *v*ia the following equation:

$$\zeta\frac{\partial\langle \boldsymbol{x}(t)\rangle_\varepsilon}{\partial t} + \boldsymbol{\Gamma}\cdot\langle \boldsymbol{x}(t)\rangle_\varepsilon = \boldsymbol{\varepsilon}, \tag{12}$$

which, for $\langle \boldsymbol{x}\,(0)\rangle_\varepsilon = 0$ yields:

$$\boldsymbol{\chi}(t) = \boldsymbol{\Gamma}^{-1}\cdot\left[\boldsymbol{I} - \exp\left(-\frac{1}{\zeta}\boldsymbol{\Gamma}t\right)\right]. \tag{13}$$

The long-time limit of the susceptibility is $\boldsymbol{\chi} = \boldsymbol{\chi}(\infty) = \boldsymbol{\Gamma}^{-1}$, so that Eq. (10) yields:

$$\left(\boldsymbol{\chi}^{-1}\cdot\boldsymbol{\sigma}\right)^{sym} = k_BT\boldsymbol{I}. \tag{14}$$

In the case of an OU process, Eq. (14) represents a generalization of the static version of the FDT, i.e. Eq. (4). The latter is recovered if $\boldsymbol{\Gamma}$ (and therefore $\boldsymbol{\chi}$ as well) is a symmetric matrix, so that we obtain:

$$\boldsymbol{\chi} = \frac{1}{k_BT}\boldsymbol{\sigma}, \tag{15}$$

or $\boldsymbol{\chi}^{-1}\cdot\boldsymbol{\sigma}/k_B = T\boldsymbol{I}$. This result is expected, as in this case detailed balance holds [6,7]. In the general case, though, Eq. (14) yields,

$$\boldsymbol{\chi}^{-1}\cdot\boldsymbol{\sigma}/k_B = T\,(\boldsymbol{I} + \boldsymbol{A})\,, \tag{16}$$

where $\boldsymbol{A}$ is a non-dimensional, antisymmetric matrix.

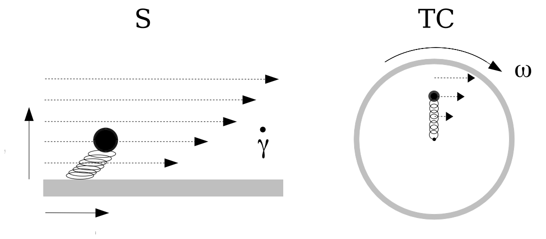

Fig. 1 – The colloidal particle attached to the spring and driven by the drag forces exerted by the velocity fields of the S (left) and TC (right) models.

Results and discussion. – The following explicit form of the damping matrix is considered:

$$\mathbf{\Gamma} = \begin{pmatrix} k_1 & -w_2 & 0 \\ w_1 & k_2 & 0 \\ 0 & 0 & k_3 \end{pmatrix} \tag{17}$$

where all the coefficients are real and $k_i > 0$ for all i, i.e., the colloidal particle is confined by a harmonic potential and driven by the drag force due to suitable velocity fields. In this case, the only non-zero terms of the $\boldsymbol{A}$ matrix are $A_{21} = -A_{12} = (w_1 + w_2) / (k_1 + k_2)$. If $w_1 = -w_2$ the $\mathbf{\Gamma}$ matrix is symmetric, $\boldsymbol{A} = \mathbf{0}$ and, as expected, FDT is ensured.

Two velocity fields are discussed in greater detail (see Fig. 1): a) simple shear flow with shear rate $\dot{\gamma}$, which we denote as S model, with $w_1 = 0$ and $w_2 = w_S = \zeta\dot{\gamma}$; b) Taylor-Couette flow inside a rotating cylinder (i.e. a rigid body rotation) with angular velocity ω, which we denote as TC model, with $w_1 = w_2 = w_{TC} = \zeta\omega$).

First, consider the static susceptibility $\boldsymbol{\chi} = \mathbf{\Gamma}^{-1}$, obtaining:

$$\chi_{xx} = \frac{k_2}{k_1 k_2 + w_1 w_2}; \qquad \chi_{yy} = \frac{k_1}{k_1 k_2 + w_1 w_2}; \qquad \chi_{zz} = \frac{1}{k_3} \tag{18}$$

On the other hand, the diagonal elements of the stationary correlation matrix $\boldsymbol{\sigma}$ are:

$$\frac{\langle x^2 \rangle}{k_B T} = \frac{k_2 (k_1 + k_2) + w_2 (w_1 + w_2)}{(k_1 + k_2)(k_1 k_2 + w_1 w_2)}; \quad \frac{\langle y^2 \rangle}{k_B T} = \frac{k_1 (k_1 + k_2) + w_1 (w_1 + w_2)}{(k_1 + k_2)(k_1 k_2 + w_1 w_2)}; \quad \frac{\langle z^2 \rangle}{k_B T} = \frac{1}{k_3}. \tag{19}$$

The above equations show that, in general, driving leads to the breakdown of the energy equipartition (with a notable exception to be discussed later).

By defining the effective static temperature $T^*_{st}(x_i) = \sigma_{ii}/k_B \chi_{x_i} = \langle x_i^2 \rangle / k_B \chi_{x_i}$ one obtains:

$$T^*_{st}(x) = T\left(1 + \frac{w_2 (w_1 + w_2)}{k_2 (k_1 + k_2)}\right) \quad T^*_{st}(y) = T\left(1 + \frac{w_1 (w_1 + w_2)}{k_1 (k_1 + k_2)}\right) \quad T^*_{st}(z) = T. \tag{20}$$

It may be proven that, if the symmetric part of $\mathbf{\Gamma}$ has positive eigenvalues, then $T^*_{st} > T/2$. Eqs. (20) prove the anisotropic violation of the static version of the FDT, i.e. Eq. (4). In fact, FDT still holds along the z axis, whereas it breaks down along the other two axis if a non-conservative driving force is present, i.e. $T^*_{st}(x), T^*_{st}(y) \neq T$ if $w_1 \neq w_2$. In particular, in the S model, $T^*_{st}(y) = T^*_{st}(z) = T$ and $T^*_{st}(x) \neq T$, while, in the TC model, with $k_1 = k_2$, one finds $T^*_{st}(x) = T^*_{st}(y) \neq T$.

Note that loosening the confinement, by making the constants $k_i, i = 1, 2$ vanishingly small, enhances the FDT breakdown. It must be also noted that the TC model with $k_1 = k_2$

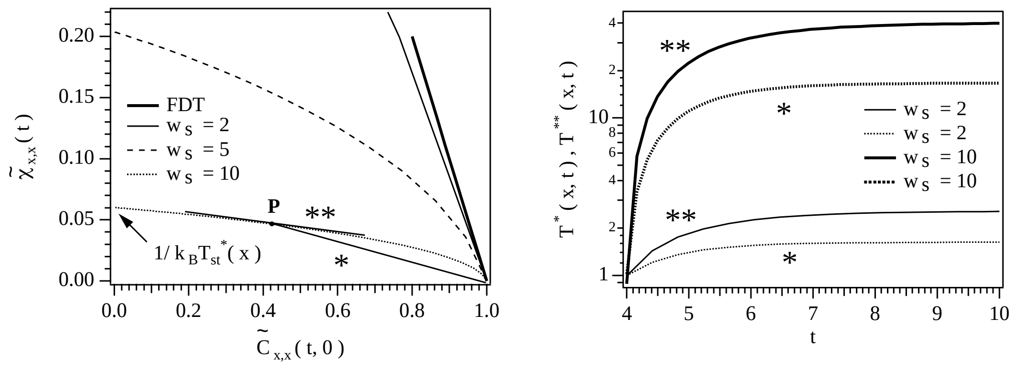

Fig. 2 – The breakdown of the FDT theorem according to the S model with $k_1/\tilde{k} = 1.2, k_2/\tilde{k} = 2, k_3/\tilde{k} = 3, T = 1$ (in units of $\tilde{k}a^2/k_B$) and different w_S values (in units of $\tilde{k}$). Time in units of $\zeta/\tilde{k}$. Left: FDT plot between the normalized correlation function $\tilde{C}_{x,x}(t,0)$ and susceptibility $\tilde{\chi}_{x,x}(t)$. The FDT theorem (bold line) holds at short times whereas it fails at long times. The slopes of the straight lines, labeled by '*' and '**', are equal to the effective temperatures of the point $\boldsymbol{P} = \{\tilde{C}_{x,x}(t',0), \tilde{\chi}_{x,x}(t')\}$, $-1/k_B T^*(x,t')$ and $-1/k_B T^{**}(x,t')$, respectively. Note that the intercept of the straight line $(*)$ on the $\tilde{\chi}_{x,x}$ axis yields $1/k_B T^*(x,t')$ and, therefore, the intercept of the curve $\tilde{\chi}_{x,x}(t)$ vs $\tilde{C}_{x,x}(t,0)$ on the $\tilde{\chi}_{x,x}$ axis yields $1/k_B T^*_{st}(x)$. Right: Time evolution of the effective temperatures $T^*(x,t)$ and $T^{**}(x,t)$ from the bath temperature $T = 1$. At long times, $T^*(x,t)$ tends to the effective static temperatures $T^*_{st}(x) = 1.63, 16.6$ for $w_s = 2, 10$, respectively. An annealing period of four time units was allowed for the initial equilibration before to switch on the non-conservative driving force.

violates the static FDT, Eqs. (20) but, according to Eqs. (19), it does not violate the equipartition of energy. **In fact, since in this case the conservative elastic force, $\boldsymbol{F}_c = -\boldsymbol{K}\cdot\boldsymbol{x} = -\nabla\phi$, with $\phi = 1/2\,\boldsymbol{x}\cdot\boldsymbol{K}\cdot\boldsymbol{x}$, is perpendicular to the non-conservative drag force, $\boldsymbol{F}_{nc} = \zeta\boldsymbol{\kappa}\cdot\boldsymbol{x}$, with $\nabla\cdot\boldsymbol{F}_{nc} = 0$, we find that the Boltzmann distribution $P = Cexp(-\phi/k_BT)$ is a stationary solution of Eq. (7).**

The dynamic version of the FDT , cfr. Eq. (3), is now considered. The correlation functions and the susceptibilities of interest are derived via Eq. (11) and Eq. (13), respectively by using standard procedures to derive both the Green function $G_{ij}(t)$ and the correlation matrix $\sigma_{ij}(t)$ [17]. The analytical expressions are rather involved and will be not reproduced here. The non-conservative driving force is applied when the system is in thermal equilibrium, i.e. the correlation matrix $\sigma_{ij}(t)$ assumes the time-independent equilibrium form and consequently, according to Eq. (11), $C_{A,A}(t,t) = C_{A,A}(\infty,\infty)$. Let us define the normalized correlation function and susceptibility as $\tilde{C}_{A,A}(t,s) = C_{A,A}(t,s)/C_{A,A}(\infty,\infty)$ and $\tilde{\chi}_{A,A}(t) = \chi_{A,A}(t)/C_{A,A}(\infty,\infty)$, respectively. One may define two effective temperatures $T^*(A,t)$ and $T^{**}(A,t)$ as [3,8],

$$T^*(A,t) = \frac{1-\tilde{C}_{A,A}(t,0)}{k_B\tilde{\chi}_{A,A}(t)}; \qquad T^{**}(A,t) = -\frac{1}{k_B}\frac{\partial\tilde{C}_{A,A}(t,0)}{\partial\tilde{\chi}_{A,A}(t)}. \tag{21}$$

For $t \to 0$, $T^*(A,t), T^{**}(A,t) \to T$, whereas for $t \to \infty$, $T^*(A,t) \to T^*_{st}(A)$. In general, the two effective temperatures are related to each other by the following relation:

$$T^{**}(A,t) = \frac{\tilde{\chi}_{A,A}(t)}{\dot{\tilde{\chi}}_{A,A}(t)}\,\dot{T}^*(A,t) + T^*(A,t), \tag{22}$$

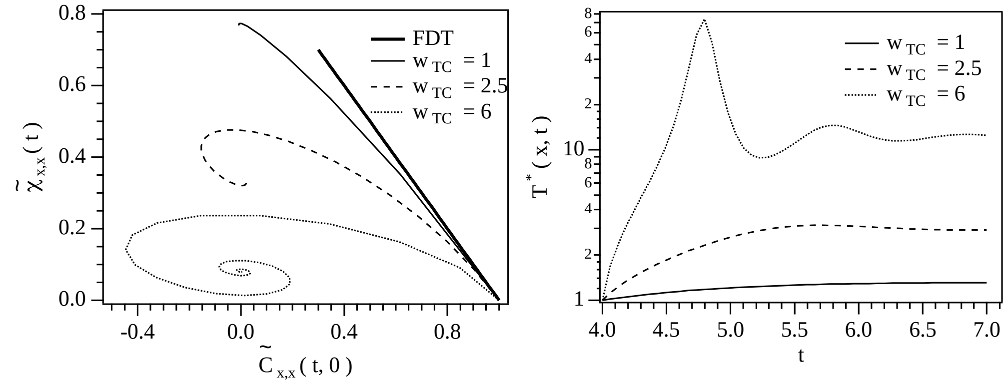

Fig. 3 – The breakdown of the FDT theorem according to the TC model. All parameters and annealing are as in Fig. 2. w_{TC} is plotted in units of $\tilde{k}$. Left: FDT plot. The FDT theorem (bold line) holds at short times, whereas it fails at long times. Right: time evolution of the effective temperature $T^*(x,t)$ from the bath temperature $T = 1$ to the effective static temperatures $T^*_{st}(x) = 1.31, 2.95, 12.25$ for $w_{TC} = 1, 2.5, 6$, respectively.

where the dot denotes time derivative.

First, the S model is discussed. Fig. 2 (left) presents the FDT breakdown on increasing the shear rate *via* the usual $\tilde{\chi}$ vs. $\tilde{C}$ plot. Similar plots are well known from numerical simulations on sheared systems [3, 8–10]. The plot also shows the geometrical interpretations of the two effective temperatures, $T^*(x,t)$ and $T^{**}(x,t)$, and the limit value $T^*_{st}(x)$ of the former. Fig. 2 (right) plots the time dependence of the two effective temperatures. At short times, as expected, they coincide with the bath temperature, whereas at long times $T^{**}(x,t) > T^*(x,t) > T$. As we have already seen, for long times, $T^*(x,t)$ tends to $T^*_{st}(x)$.

The TC model is now discussed. Fig. 3 (left) presents the FDT breakdown on increasing $w_{TC} = \zeta\omega$, showing that, unlike the previous case, plots here are characterized by spiralling patterns. Fig. 3 (right) shows the time dependence of the effective temperature $T^*(x,t)$. It starts from the bath temperature and approaches the limit value $T^*_{st}(x)$ at long times. It must be noted that for large w_{TC} values, i.e. large angular frequencies, $T^*(x,t)$ becomes negative in some time region. However, a time τ always exists such as $T^*(x,t) > 0$ for $t > \tau$. This is also signaled by the fact that, according to Eq. (20), $T^*_{st}(x) > 0$. The FDT plot suggests that $T^{**}(A,t)$ is not a convenient choice for the TC model. Indeed, Fig. 4 shows that this is the case. It compares $T^*(x,t)$ and $T^{**}(x,t)$. For $4w^2_{TC} > (k_1 - k_2)^2$ the latter has a strong oscillatory character with divergencies occurring with period $2\pi[4w^2_{TC} - (k_1 - k_2)^2]^{-1/2}$.

How large is the FDT breakdown by trapping a driven colloidal particle ? Let us consider the case of optical tweezers [18]**. The stiffness k of the trap depends on its design and the size of the particle, but a value of $k \simeq 50\,pN/\mu m$ is reasonable. From Eqs. 20 with $a = 300\,\mu m, \eta = 76\,mPa \cdot s, \dot{\gamma} = 0.2\,s^{-1}$** [19] **the S model yields $T^*_{st}(x) \cong 2.48T$. For the TC model with $\omega = 0.2\,rad/s$ one gets $T^*_{st}(x) \cong 3.96T$.**

In conclusion, we presented a class of models describing the motion of colloidal particles being confined in a harmonic well and dragged by a shear flow. Our results expose the role of the detailed balance to ensure the validity of FDT [6, 7] and shows that the violation of FDT is manifested through the appearance of an antisymmetric temperature operator. **It is found that the effective temperature defined by the static FDT is always well defined, whereas for Taylor-Couette flow the one drawn by the time-dependent**

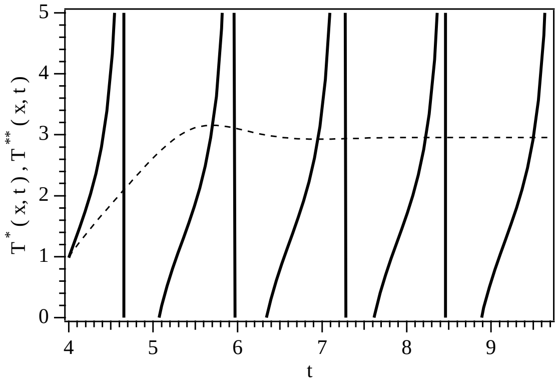

Fig. 4 – Comparison of the time evolution of the effective temperatures $T^{*}(x,t)$ (dashed line) and $T^{**}(x,t)$ (thick line) for the TC model . All parameters and annealing as in Fig.2. $w_{TC}/\tilde{k} = 2.5$. Both the effective temperatures start from the bath temperature. $T^{*}(x,t)$ tends to $T^{*}_{st}(x) = 2.95$. $T^{**}(x,t)$ oscillates between positive and negative values.

FDT is *meaningless*, thus suggesting that the former is more physically sound. In addition, it is shown that energy equipartition is not sufficient to ensure the validity of FDT, while, as expected, loosening confinement enhances FDT violations. **Optical traps are a convenient tool to test the above models.**

* * *

Financial support from MIUR within the PRIN project "Aging, fluctuation and response in out-of-equilibrium glassy systems" is gratefully acknowledged.

REFERENCES

[1] Cugliandolo L. F., Kurchan J. and Peliti L., *Phys. Rev. E*,**55** (1997) 3898.
[2] Casas-Vazquez J. and Jou D., *Rep. Prog. Phys.*, **66** (2003) 1937.
[3] Kurchan J., *Nature (London)*, **433** (2005) 223.
[4] Santamara-Holek I. , Reguera D. , and Rub J. M., *Phys.Rev.E.* **63** (2001) 051106.
[5] Fielding S. and Sollich P., *Phys.Rev.Lett.* **88** (2002) 050603.
[6] Harada T. and Sasa S.-I., *Phys.Rev.Lett.* **95** (2005) 130602.
[7] Speck T. and Seifert U. , *Europhys. Lett.* **74** (2006) 391.
[8] Crisanti A. and Ritort F, *J.Phys.A: Math.Gen.*,**36** (2003) R181.
[9] Berthier L. and Barrat J.-L., *J. Chem. Phys.*,**116** (2002) 6228.
[10] O'Hern C.S., Liu A.J. and Nagel S.R., *Phys.Rev.Lett.* **93** (2004) 165702.
[11] Bellon L. , Ciliberto S. and Laroche C., *Europhys. Lett.* **53** (2001) 511.
[12] Abou B. and Gallet F., *Phys.Rev.Lett.* **93**, (2004) 160603.
[13] Kurchan J. and Makse H.A., *Nature (London)*, **415** (2002) 614.
[14] Szamel G., *Phys.Rev.Lett.* **93** (2004) 178301.
[15] Callen, H.B. and Green, R.K., *Phys.Rev.* **86** (1952) 702, 1387.
[16] Brady J.F., *J. Chem. Phys.*,**99** (1993) 567.
[17] Risken H., *The Fokker-Planck Equation*, (Springer, Berlin, 1984).
[18] Neuman K. C. and Blocka S. M. , *Rev. Sci. Instrum.*,**75** (2004) 2787.
[19] Lee M. , Alcoutlabi M. , Magda J. J. , Dibble C., Solomon M. J. , Shi X. , McKenna G. B. , *J. Rheol.*,**50** (2006) 293.